
Article:
Marki, P.Z., Kennedy, J.D., Cooney, C.R. orcid.org/0000-0002-4872-9146 et al. (2 more authors) (2019) Adaptive radiation and the evolution of nectarivory in a large songbird clade. Evolution, 73 (6). pp. 1226-1240. ISSN 0014-3820

https://doi.org/10.1111/evo.13734

Adaptive radiation and the evolution of nectarivory in a large songbird clade

ABSTRACT

The accumulation of exceptional ecological diversity within a lineage is a key feature of adaptive radiation resulting from diversification associated with the subdivision of previously underutilized resources. The invasion of unoccupied niche space is predicted to be a key determinant of adaptive diversification, and this process may be particularly important if the diversity of competing lineages within the area in which the radiation unfolds is already high. Here, we test whether the evolution of nectarivory resulted in significantly higher rates of morphological evolution, more extensive morphological disparity, and a heightened build-up of sympatric species diversity in a large radiation of passerine birds (the honeyeaters, ca. 190 species) that have diversified extensively throughout continental and insular settings. We find that a large increase in rates of body size evolution and general expansion in morphological space followed an ancestral shift to nectarivory, enabling the build-up of large numbers of co-occurring species that vary greatly in size compared to related and co-distributed non-nectarivorous clades. These results strongly support the idea that evolutionary shifts into novel areas of niche space play a key role in promoting adaptive radiation in the presence of likely competing lineages.

Keywords: character displacement, macroevolution, macroecology, species richness, key innovations, morphological evolution

INTRODUCTION

Adaptive radiation describes the scenario in which lineage diversification is coupled with extensive ecological divergence into a wide variety of niches (Osborn 1902; Huxley 1942; Simpson 1953; Schluter 2000a). Although some iconic adaptive radiations have been extensively studied by evolutionary biologists (e.g. Darwin's finches, Hawaiian honeycreepers and Caribbean anoles), our general understanding of the factors that promote this phenomenon remain incomplete (Schluter 2000a). Ecological opportunity in the form of new and/or underexploited resources is believed to be a common prerequisite for adaptive radiation, but this may arise in a multitude of ways. For example, ecological opportunity may emerge as a consequence of (i) the colonization of new geographic areas, (ii) the appearance of a new resource, (iii) the extinction of competitors/predators, or (iv) as a result of the evolution of key innovations (Simpson 1953; Schluter 2000a; Losos and Mahler 2010; Stroud and Losos 2016). Most well-studied adaptive radiations have resulted from the colonization of geographically isolated areas and are therefore likely to have unfolded in the absence of competition from closely related lineages (Losos 2010; Soulebeau et al. 2015; Stroud and Losos 2016). Much less is known about the factors facilitating adaptive radiation when the levels of species diversity among potentially competing lineages is already high. This scenario is particularly applicable to radiations occurring throughout continental settings, where the bulk of the world's species diversity is distributed. In these instances, one important factor is thought to be the evolution of new morphological and physiological traits that allow lineages to utilize novel resources, and radiate free from competition with related co-occurring species (Miller 1949; Simpson 1944; Hunter 1998; Rabosky 2017).

The evolution of traits that facilitate access to previously inaccessible resources has been hypothesized to underlie the evolutionary success of many large radiations, with proposed examples including the evolution of phytophagy in insects (Mitter *et al*. 1998), or the pharyngeal

jaw in labroid fishes (Liem 1973; Galis and Drucker 1996). Under this scenario, lineages that are able to invade unoccupied niche space, are predicted to undergo increased rates of trait evolution and exhibit greater ecological disparity compared to related clades, assuming that the available resources are amenable to further subdivision (Futuyma 1998; Losos and Mahler 2010; Rabosky 2017). Moreover, such clades should also be characterized by a shift in ecological positioning relative to the background clade, as may be evidenced by the evolution of new traits (or trait combinations) that facilitate novel patterns of resource utilization (Rabosky 2017). Adaptive radiations that unfold in this way may also be expected to support higher numbers of species at smaller spatial scales, as greater ecological divergence facilitates a high degree of sympatry among the constituent taxa (Schluter 1996). The invasion of underexploited areas of niche space through the evolution of novel traits has also in some instances been proposed to result in increased lineage diversification (Mitter et al. 1988; Slowinski and Guyer 1993; Hodges and Arnold 1995; Bond and Opell 1998). However, this hypothesis remains contentious as the evolution of such traits may increase the overall diversification of the parent clade (thus raising its accumulated species richness), without necessarily increasing rates of lineage diversification among the innovative clade (Rabosky 2017). However, empirical assessments of these predictions, and documentation of the tempo and mode by which radiations of this nature unfold, are currently limited. We address these issues by assessing the effect of an ancestral shift in diet on rates of morphological evolution, lineage diversification and patterns of species co-occurrence within a large clade of passerine birds that has radiated extensively throughout continental and insular settings.

The infraorder Meliphagides is a passerine radiation of approximately 290 species distributed across Australasia and the Indo-Pacific (Gardner et al. 2010; Marki et al. 2017). Australasia is thought to represent the ancestral area of songbird (oscine passerines) diversification (Barker et al. 2004; Jønsson et al. 2011; Moyle et al. 2016), thus providing a contrasting geographic

setting to other studies of adaptive radiations that have predominantly assessed these trends in isolated and species depauperate island environments (Pratt 2005; Grant and Grant 2008; Losos 2009). Ecological and phenotypic diversity is particularly pronounced in the honeyeater subclade (family Meliphagidae), which comprises ca. 65% (187 species) of the overall species richness of the infraorder. Honeyeater species possess a number of unique morphological and physiological adaptations for nectarivory, including structural modifications to the renal system for more efficient balancing of fluid intake and a brush-tipped protrusible tongue (Paton and Collins 1989; Cassoti and Richardson 1992; Goldstein and Bradshaw 1998a,b). These adaptations are hypothesized to have allowed honeyeaters to successfully exploit a novel food source (nectar) and radiate into areas of ecological niche space that were previously unoccupied in this geographic setting (Keast 1976; Miller et al. 2017). Together, these factors make the Meliphagides an ideal study system for investigating the dynamics of adaptive radiation at large geographic scales.

Here, we use empirical data to assess core, but largely untested predictions of adaptive radiation theory following the invasion of novel niche space. First, we test the prediction that following the evolution of nectarivory honeyeaters should occupy a unique and exceptionally diverse part of morphological space compared to other co-distributed and closely related passerine clades. Second, we evaluate whether the macroevolutionary dynamics of trait evolution in nectarivorous lineages are decoupled from those of non-nectarivorous lineages. Finally, having established such a link, we examine whether these processes have influenced lineage diversification dynamics, geographic variation in species richness and the functional diversity of Meliphagoid assemblages.

MATERIALS AND METHODS

95 *Phylogenetic, morphological and ecological data*

96 We used the recently published molecular phylogeny of the Meliphagides by Marki et al. (2017) in
97 all analyses. This phylogeny is nearly complete at the species-level and includes 286 of 289 (99%)
98 of the currently recognized species according to the IOC World Bird List version 6.2 (Gill and
99 Donsker 2016). The phylogeny was calibrated using a combination of fossils and secondary
100 calibration points, and was summarized as a maximum clade credibility (MCC) tree upon which all
101 comparative analyses were performed, unless otherwise stated .

102 To quantify morphological variation among the Meliphagides, we collected data on
103 seven ecologically relevant traits that represent major aspects of external avian anatomy, from
104 museum study skins. We measured tarsus length, hind toe length (including claw), wing length,
105 Kipp's distance and bill length, width and depth (Table S1). Male specimens were measured where
106 possible, although in a few cases when these were unavailable in the respective collections, the
107 measurements for these species were supplemented with those from females or unsexed specimens.
108 We obtained measurements for a total of 1,245 individual specimens including all but 13 taxa
109 represented in the phylogeny (the species for which we were not able to obtain morphological data
110 were *Acanthiza katherina*, *Amytornis ballarae* and *A.dorotheae*, *Aphelocephala pectoralis*,
111 *Bolemoreus hindwoodi*, *Chenorhamphus campbelli*, *Lichmera monticola*, *Manorina melanotis*,
112 *Meliphaga cinereifrons* and *M. fordiana*, *Myzomela blasii*, *Ptiloprora mayri*, *Stipiturus mallee* and
113 *ruficeps*), with an average of 4.5±1.9 SD specimens measured per species. In addition to the
114 Meliphagides, we also collected morphological measurements for the majority of species within 13
115 families that are co-distributed with the honeyeaters (Artamidae, Campephagidae, Cinclosomatidae,
116 Climacteridae, Corvidae, Melanocharitidae, Monarchidae, Oriolidae, Pachycephalidae,
117 Paradisaeidae, Petroicidae, Ptilonorhynchidae and Rhipiduridae) totaling 398 additional species
118 (2,085 specimens measured, mean per species = 5.2±1.6 SD). Using ANOVA across the full

morphological data set, we found that between-species variance on average accounted for 98% (range 96 – 99%) of the variance across all seven traits. Consequently, all subsequent analyses were performed on the log-transformed mean trait values calculated for each individual species. The MCC tree and the morphological measurements from the individual specimens have been made available on the Dryad online repository (hyperlink to be provided upon acceptance).

We discretely classified individual meliphagoid species according to whether or not they include nectar in their diets using information from a large database of ecological traits (Wilman et al. 2014). For species not included in the Wilman et al. (2014) diet database but present in the phylogeny (n = 13), we used the most frequent condition among members of the genus to represent their dietary category.

Analyses of trait evolution

To assess the evolutionary origins of nectarivory among the Meliphagides, we reconstructed ancestral diets using stochastic character mapping (Bollback 2006) implemented in the R package *phytools* (Revell 2012; R Core Team 2016). To do this, we first compared two models of variation in transition rates among states bycomputing the likelihoods of an equal-rates (ER) and an all-rates different (ARD) model to our data. Likelihood ratio tests indicated that the more complex ARD model did not represent a significantly better fit than an ER model (P = 0.31) and therefore we consequently estimated 1,000 stochastic character maps using the ER model. To test the hypothesis that honeyeaters occupy distinct and extended parts of morphological space relative to co-distributed clades we used a number of different approaches. First, in order to compare the morphological diversity of honeyeaters (n = 180 species) with that of the four remaining meliphagoid families (n = 93 species, herein we refer to these clades as the 'background

meliphagoids'), we performed a phylogenetic principal component (pPC) analysis upon the covariance matrix of the seven log-transformed variables (Revell 2009). Second, we also assessed the morphological space occupied by honeyeaters to that of a broader subset of the Australasian/Indo-Pacific avifauna that encompassed the background meliphagoids, in addition to the members of 13 further passerine families present in the region (n = 491 species, herein we refer to this assemblage of clades as the 'regional passerines'). For this analysis, we used the species scores generated from a separate principal component analysis of the log-transformed morphological measurements. Due to the lack of comprehensive molecular phylogeny for this wider species set, we were unable to correct for the influence of shared ancestry in this analysis. Combined, PC axes 1-4 explained 95% of the overall variance in both the phylogenetic and non-phylogenetic PCAs (Table S2-3), and we thus focused our subsequent analyses and interpretations on these variables. To test whether honeyeaters occupy unique parts of morphological space compared to the background meliphagoids and the regional passerine fauna, we estimated the four dimensional hypervolumes of honeyeaters relative to related clades, using the *hypervolume* methodology (Blonder et al. 2014). We thus performed two sets of comparisons using the first four PCA axes derived from the separate pPC and PC analyses described above (honeyeaters versus background meliphagoids, and honeyeaters versus regional passerines). The hypervolumes were estimated using a multidimensional kernel estimation procedure, and bandwidths that were determined using the Silverman bandwidth estimator (Blonder et al. 2015). Overlap in the hypervolumes between the clades in the two sets of analyses was calculated using the Sørensen index (see Blonder et al. 2015), whereby a value of 0 indicates no overlap between the hypervolumes, and a value of 1 indicates identical hypervolumes. Finally, to further assess whether honeyeaters occupy unique parts of morphological space and to define specific traits that differentiate the groups, we performed a linear discriminant analysis upon the seven original log-

166 transformed morphological measurements, treating the regional passerine clades as both a single
167 class, and as multiple classes divided by family.

168 The invasion of novel niche space has been predicted to result in a decoupling of rates
169 of eco-morphological evolution between the invading and non-invading clades (Rabosky 2017). To
170 test this hypothesis, we compared the relative fit of different models of trait evolution using the R
171 package *mvMORPH* (Clavel et al. 2015). Specifically, we compared a Brownian motion (BM)
172 model with a single rate of trait evolution for all lineages (BM1) to a BM model with separate rates
173 of trait evolution for nectarivorous and non-nectarivorous lineages (BMM). We fit these two models
174 to each of the 1,000 stochastic character maps. Univariate analyses were run for each of the first
175 four pPC axes (pPC1-4). Similarly, we also compared models of multivariate evolution (pPC1-4)
176 across ten evenly sampled stochastic character maps. Model support was assessed using AICc
177 scores and Akaike weights. To test for the possible influence of phylogenetic uncertainty, we
178 repeated the above analyses across a posterior distribution of 1,000 Meliphagides trees obtained
179 from the study of Marki et al. (2017) upon which we first estimated stochastic character maps using
180 a single simulation per tree. In addition, we also assessed finer scale lineage variation in the tempo
181 and mode of meliphagoid morphological evolution using a variable rates model as implemented in
182 BayesTraits v2 (available from http://www.evolution.rdg.ac.uk/). This approach uses reversible-
183 jump Markov chain Monte Carlo algorithms (rjMCMC) and two scaling mechanisms to identify
184 rate changes along single branches and for whole clades across the phylogeny (Venditti et al. 2014).
185 We used default priors for the phylogenetic mean (α) and Brownian variance (σ) parameters and ran
186 a single rjMCMC chain for each of the four pPC axes for 50 million generations, sampling every
187 5000th generation. In addition, we ran a correlated multivariate analysis that assessed the
188 evolutionary dynamics of all four axes simultaneously, using the same parameters. We assessed
189 mixing and convergence of the chains, before the first 5 million generations were removed as a

burn-in. BayesTraits outputs a posterior distribution of trees in which the branches are scaled by the rate of evolutionary change that best explain the distribution of the trait values at the tips. Results were summarized by (i) calculating the mean rate of trait evolution along each branch, considering the posterior distribution of trees, and (ii) by calculating the posterior probability of branch or clade shifts over all samples for each node in the tree. To account for uncertainty in the precise location of rate shifts across posterior samples, we calculated the posterior probability of a rate shift as the sum of the probability of this having occurred on a focal node, or on either of the descendant nodes (following Cooney et al. 2017). In addition to BayesTraits, we also investigated another widely used framework for inferring variable rates of trait evolution across a phylogeny (BAMM v2.5.0; Rabosky 2014; Rabosky et al. 2014a). The BAMM method attempts to identify the location and number of distinct macroevolutionary rate regimes on the phylogeny. The number of distinct regimes are modelled following a Poisson distribution, with rjMCMC used to sample different regimes that best explain the distribution of trait values at the tips of the tree. We used the R package *BAMMtools* (Rabosky et al. 2014b) to estimate the prior settings for the phenotypic rates and for the hyperprior on the Poisson rate prior. The rjMCMC chains were run for 10 million generations each, sampling every 1000^{th} generation. Convergence and mixing of the individual chains was assessed through visual inspection and by computing effective sample sizes (ESS), with the first 10% of samples subsequently discarded as a burn-in. We analyzed each of the four pPC axes calculated for the Meliphagides using the MCC tree as input.

To compare model performance between alternative evolutionary methods, we used the approach outlined in Cooney *et al*. (2017) that builds on the methodological developments of Pennell et al. (2015) and Chira and Thomas (2016), to calculate log-likelihoods describing the relative fit of different models of continuous trait evolution to each pPC axis. These analyses were performed using the *fitContinuous* function in the R package *geiger* (Harmon et al. 2008). We thus

calculated the likelihood of three single-process models (Brownian motion (BM), Ornstein-Uhlenbeck (OU) and early-burst (EB)) fitted to the original untransformed tree, and compared these to the likelihoods of BM models fit to the mean rate-transformed trees derived from BAMM (obtained using the function *getMeanBranchLengthTree* in *BAMMtools*) and BayesTraits. Model comparisons (using delta log-likelihoods) indicated that BayesTraits represented a significantly better description of the patterns of morphological evolution among the Meliphagides than either BAMM or any of the single-process models for all pPC axes analyzed (pPC1-4, Table S4). Consequently, we focus our interpretation and discussion on the BayesTraits results (although those generated by BAMM were largely congruent, Fig. S1).

To test whether the evolution of nectarivory by honeyeaters has led to an increase in the total volume of eco-morphological space occupied by the Meliphagides (Rabosky 2017), we assessed the accumulation of morphological disparity and the filling of morphospace through time. Using maximum likelihood in *phytools* (Revell 2012), we reconstructed ancestral states for each of the pPC axes using the mean rate-transformed trees from BayesTraits. We then divided the tree in time slices at 0.5 million year intervals, starting at the root, and for each time slice extracted ancestral state estimates for all lineages present at a given time. We compared both disparity accumulation of the individual PC axes, and for all axes combined, by summing the variances across all four axes. Finally, we compared the empirical accumulation of trait disparity through time, with that expected under a constant-rate BM model and a variable-rates (VR) model of trait evolution. Thus, for both null models we simulated 500 replicate datasets for each of the pPC axes and for pPC1-4 combined, to calculate disparity through time curves.

Lineage diversification and spatial diversity patterns

237 The invasion of novel or unoccupied niche space may in some instances lead to a decoupling in
238 diversification dynamics between the invading and non-invading clades (e.g. Mitter et al. 1988, but
239 see Givnish 2015; Rabosky 2017). To test for a decoupling in the dynamics of lineage
240 diversification between nectarivorous and non-nectarivorous lineages we applied the hidden-state
241 speciation and extinction framework (HiSSE; Beaulieu and O'Meara 2016). The HiSSE framework
242 is an extension of the binary-state speciation and extinction model (BiSSE; Maddison et al. 2007)
243 developed to circumvent issues of high type I error rates associated with this method (Rabosky and
244 Goldberg 2015). Using HiSSE, we compared the fit of five different models of lineage
245 diversification (see Table S5 for details of number of parameters and constraints for each model),
246 accounting for incomplete taxon sampling (3/289 species missing). Given the difficulty in reliably
247 estimating transition rates in these analyses (Beaulieu and O'Meara 2016), we set transition rates
248 between diet categories to be equal across all models. Model support was assessed using AICc
249 scores and Akaike weights, and the results were visualized using model-averaged marginal
250 reconstructions of diet and net diversification rates.

251 To assess whether increased ecological dispersion among honeyeaters has led to a
252 heightened accumulation of sympatric species diversity (Schluter 1996), we compared the
253 geographic species richness patterns of the honeyeaters to that of the background meliphagoids. To
254 do this, we obtained range maps from a global distributional database (Rahbek and Graves 2001;
255 Rahbek et al. 2012), with species ranges recorded at a resolution of 1° × 1°. We then mapped the
256 species richness of the honeyeaters and the background meliphagoids by overlaying the ranges,
257 before summing the number of species present in each 1° grid cell. Subsequently, we assessed the
258 range and standard deviation of the individual pPC axes throughout all grid cells among both
259 groups. Using linear models, we regressed the grid cell values of the species richness of the
260 honeyeaters against the background meliphagoids. Finally, we determined how the range and

standard deviation of the pPC axes varied among the honeyeaters and background meliphagoids as a function of the species richness of all grid cells. As the range can be sensitive to outlying values, we also mapped the 95% quantiles of the range in pPC1-4 to explore the robustness of our results.

RESULTS

Diet reconstructions and morphological diversity

The ancestral reconstruction of the presence of nectar in the diet of the Meliphagides is strikingly characterized by a shift from a non-nectarivorous diet to one that can incorporate nectar in the common ancestor of honeyeaters (Fig. 1a). Nectarivory has also evolved independently among the pardalotes (family Pardalotidae) and among a handful of species of Australasian warblers (family Acanthizidae) that are members of the background meliphagoids. Among honeyeaters, loss of nectarivory has occurred independently on a number of more terminal branches, such as in the largely frugivorous genera *Melipotes* and *Macgregoria*, as well as in more insectivorous genera such as *Epthianura* and *Timeliopis*. A pPCA of the seven log-transformed morphological traits (Table S1) comparing honeyeaters against background meliphagoids, showed that the first axis (pPC1) strongly reflected overall size, explaining 65.3% of the total variance in the morphological measurements (Table S2). The next three axes (pPC2-4) were related to variation in Kipp's distance (pPC2), bill depth and width (pPC3), and bill length (pPC4) respectively, together explaining 29.8% of the variance. Visual comparisons of species scores on pPC axes 1-4 highlight the great morphological disparity and distinctiveness of the honeyeaters. First, the extent and variance of body sizes (pPC1) exhibited by honeyeaters is much greater than that of the background meliphagoids (Fig. 2a). Although differences in shape variance are less extensive, honeyeaters generally have higher values of pPC2, in part, reflecting their greater Kipp's distance values (Fig.

2b). In addition, honeyeaters largely cluster separately from the background meliphagoid groups on pPC4, which is primarily related to differences in relative bill length (Fig. 2b). Results of a second, phylogenetically uncorrected PCA analysis comparing honeyeaters against the regional passerine fauna are largely congruent with these findings (Table S3), with honeyeaters exhibiting a high diversity of body sizes (Fig. 2c) and unique morphologies related to bill shape and length (PC3-PC4) (Fig. 2d).

The four dimensional hypervolume comparisons strongly support the above findings, with the Sørensen index indicating limited morphological overlap between the honeyeaters and background meliphagoids (Fig. S2, Sørensen's index = 0.07), and between the honeyeaters and regional passerines (Fig. S3, Sørensen's index = 0.22). Moreover, honeyeaters were found to occupy a high fraction of unique morphological space relative to both background meliphagoids and to the broader regional passerine fauna (0.93 and 0.47 of the overall morphospace respectively). A linear discriminant analysis of the seven original log-transformed measurements are in congruence with these results, illustrating that honeyeaters occupy distinct parts of morphological space relative to other regional passerines, with more than two-thirds of honeyeater species correctly classified as members of the family. Group means on the single discriminant axis were -1.51±0 .93 for honeyeaters and 0.56±1.03 for the remaining regional passerine species (Fig. S4). Normalized canonical coefficients separating the two groups indicate that the distinctiveness is largely driven by the comparatively long and narrow bills of the honeyeaters relative to other regional passerines (Table S6). Similar results were obtained from a comparison of honeyeaters against the regional passerine clades when these were divided by family, with 89% of honeyeaters correctly classified (Table S7).

307 *Morphological evolution*

308 Comparisons of different models of trait evolution using *mvMORPH* provided strong support for a
309 decoupling of trait diversification dynamics among nectarivorous and non-nectarivorous lineages.
310 Models with separate rates of trait evolution (BMM) for nectarivorous and non-nectarivorous
311 lineages represented the best-fitting model for pPC1, pPC2, pPC4 and the multivariate analysis of
312 pPC1-4, whereas a single-rate BM (BM1) model was the best fit for pPC3 (Table 1). For pPC1,
313 pPC4 and pPC1-4 nectarivorous lineages were found to have a higher rate of evolution than non-
314 nectarivorous lineages. For pPC2, nectarivorous lineages were found to have a lower rate of
315 evolution than non-nectarivorous lineages. These results were largely corroborated when
316 phylogenetic uncertainty was accounted for (Table S8), although support for a single-rate BM
317 (BM1) model was only marginally better than a BMM model for the analysis of pPC3.

318 The BayesTraits analyses of the multivariate data (pPC1-4 combined) recovered a
319 number of rate shifts distributed across the Meliphagides (Fig. S5), including a substantial single-
320 branch shift on the stem branch of the honeyeaters (PP = 0.73), as well as several rate shifts on
321 more terminal branches and nodes among both honeyeaters and background meliphagoids.
322 Deconstructing these trends among the individual pPC axes provided strong support for a clade-
323 wide shift to higher rates of trait evolution near the base of the honeyeater clade on pPC1 (PP =
324 0.90; Fig. 1b, S5) and for three species of *Gerygone* among the background meliphagoids (PP =
325 0.83). No rates shifts in the univariate analysis of pPC2-4 were strongly supported (all PP < 0.7).

326 Analyzing the accumulation of morphological disparity through time, we find that
327 disparity has steadily accumulated across the Meliphagides when considering all pPC axes
328 congruently (Fig. S6-8). Focusing on the individual pPC axes, we show that that this pattern is
329 largely driven by an expansion in size disparity (pPC1) among the honeyeaters (Fig. 1c). Whereas

body size disparity has continued to increase throughout the evolutionary history of the honeyeaters, this has not been the case for the background meliphagoid lineages, which have accumulated more limited disparity overall (Fig. 1c). Disparity accumulation on pPC2 exhibits a contrasting trend, however, with an early increase in disparity among the background meliphagoids, followed by two periods of relative stasis towards the present. Although the background meliphagoids have accumulated higher total disparity on pPC2 than the honeyeaters, both groups have continued to accumulate disparity through time on this axis. Disparity accumulation on pPC3 exhibit similar trends to that of pPC1, being characterized by continual accumulation of disparity towards the present (Fig. S6-8). For pPC4, the disparity accumulation of the overall Meliphagides is characterized by an early expansion in disparity, followed by relative stasis, reflecting the divergence in bill morphology between the honeyeaters and the background meliphagoids. Following the occupation of unique areas of morphospace, disparity accumulation among the honeyeaters and background meliphagoids is comparatively less extensive and is dominated by a largely continuous and constant accumulation of disparity through time. Comparing the above trends to null expectations based on constant-rate (BM) and variable-rates (VR) models, suggest that disparity accumulation among meliphagoid lineages is largely consistent with a process of continuous niche expansion, with the possible exception of overall meliphagoid and background meliphagoid disparity accumulation on pPC2, and overall meliphagoid disparity accumulation on pPC4 which for both axes show signatures of slowdowns in disparity and thus niche expansion towards the present.

Lineage diversification and spatial diversity patterns

An analysis of lineage diversification dynamics using HiSSE suggested that a model with speciation rate variation associated with a hidden trait was the most strongly supported (AIC weight = 0.67, Table S5). An alternative model where in addition, extinction rates were also free to vary between the two hidden states also received substantial support (AIC weight = 0.24). Models where speciation rate variation was associated with diet, received little support (AIC weight < 0.03). Mapping model-averaged marginal reconstructions of diet and speciation rates onto the Meliphagides tree suggests that rates of speciation are generally high, with the exception of certain lineages that have lower rates, including the bristlebirds (Dasyornithidae), goldenface and fernwren (*Pachycare flavogriseum* and *Oreoscopus gutturalis*), and two species of Sulawesi honeyeaters (*Myza*) (Fig. S9).

Analyzing spatial diversity patterns, we found that honeyeaters exhibit geographic gradients of species richness that are highly correlated with the overall pattern shown by the background meliphagoid clades (Fig. 3a and 4a, $R^2 = 0.65$ where richness of either group ≥1). Furthermore, both groups almost completely overlap in the range of their overall distribution, with the highest levels of grid cell richness being found in eastern Australia and New Guinea (Fig. 3a). However, the absolute richness of the honeyeaters (max richness = 42, mean richness = 10.5±7.5 SD) is substantially higher than that of background meliphagoids (max richness 25, mean richness = 6.9 ± 6.2 SD) across the majority of grid cells in which the groups co-occur. To assess how species richness patterns compare with those of morphological diversity, we mapped the range and standard deviation of the individual pPC axes across grid cells (Fig. 3b-c; Fig. S10). First, we find that honeyeaters have a higher diversity of body sizes (pPC1) across grid cells compared to the background meliphagoids (Fig. 3b-c), with both continental areas (e.g. eastern Australia and New Guinea) and islands (e.g. New Caledonia and Manus) standing out as areas harboring exceptional body size diversity, results that are robust to the exclusion of outliers (Fig. S11). Thus, for a given

level of grid cell richness, both the range and standard deviation of body size is greater among the honeyeaters in contrast to the background meliphagoid groups (Fig 4b-c, Fig. S12). Conversely, for pPC2 the background meliphagoid groups show a higher range and standard deviation within grid cells. For pPC3-4, we find that within grid cells, the honeyeaters and background meliphagoid groups overlap extensively in the range and standard deviation of the values of their co-occurring species (Fig. S10). Thus, unlike our findings for pPC1, the geographic patterns of range and standard deviation among pPC2-4 do not reflect the underlying gradients in species richness.

DISCUSSION

The invasion of novel ecological niche space has been hypothesized to underlie the adaptive diversification of a wide range of organismal groups, but the role of this process in generating species and phenotypic diversity across large geographic scales remains poorly known. In this study, we tested key predictions of this hypothesis by analyzing the effects of an extensive shift in diet and resource use among a large continental and insular radiation of passerine birds – the honeyeaters. By explicitly analyzing these trends in a phylogenetic context that includes the honeyeaters and their closest relatives, we find strong evidence that the evolution of nectarivory represented the exploitation of underutilized ecological space that has coincided with substantial increases in the rate of morphological evolution, leading to the accumulation of extensive morphological disparity. Analyses of morphological evolution provide evidence for a clade-wide shift to substantially higher rates of body size evolution within the honeyeaters (Fig. 1B; Fig. S1; Table 1). The increase in rates of body size evolution followed a major change in diet that evolved to encompass nectar (Fig. 1A), allowing honeyeaters to enter novel regions of niche space in comparison to the regional passerine fauna with which they co-occur. However, this significant

399 dietary shift did not lead to a decoupling (i.e. acceleration or deceleration) of the dynamics of
400 speciation among the honeyeaters and the background meliphagoids (Fig. S9, Table S5).
401 Conversely, analyses of spatial diversity patterns suggest that despite having converged on
402 congruent geographic diversity patterns, honeyeaters exhibit consistently higher levels of body size
403 diversity and species richness than their close relatives within 1° grid cells (Fig. 3-4). These
404 findings suggest that a shift towards nectarivory positively influenced the capacity of the
405 honeyeaters to accumulate high sympatric species diversity. Extensive diversification along the
406 body size axis could enable a greater number of honeyeater species to co-exist, reflecting their entry
407 into an unoccupied adaptive zone (nectarivory) that allowed honeyeaters to fill vacant ecological
408 and morphological space. Together, our findings highlight the important role that evolutionary
409 innovation and the invasion of novel ecological niche space play in generating extensive ecological
410 diversity and the build-up of sympatric species diversity throughout large geographic areas.

411 Character displacement resulting from interspecific competition for resources is
412 believed to be the main driver of ecological and phenotypic disparification in adaptive radiation
413 (Simpson 1953; Schluter 2000a,b; Losos and Mahler 2010). For honeyeaters, size-related
414 aggression and displacement within flowering trees is a well-known phenomenon and assumed
415 driver of body size evolution (Paton and Ford 1983; Diamond et al. 1989). This hypothesis provides
416 a possible explanation for the tight congruence between the shift towards a nectarivorous diet and
417 the increase in rates of body size evolution and disparity accumulation in the group. Honeyeaters
418 are notorious for their aggressiveness, and even Alfred Russel Wallace noted how friarbirds would
419 ferociously defend flowering trees against potential competitors (Wallace 1869). Although mimicry
420 may be one tactic to avoid attack from larger species (Diamond 1982; Prum 2014), positive
421 selection for smaller body size may represent another viable scenario, as small birds may be able to
422 utilize resources that are inaccessible or not easily monopolized by larger birds (e.g., on small

423 terminal twigs in outer parts of a tree), thus avoiding aggressive attacks (Diamond et al. 1989).
424 Interestingly, our findings of rapid and extensive body size evolution among honeyeaters are in
425 stark contrast to the two other major nectarivorous clades of birds – the hummingbirds and sunbirds
426 – which exhibit comparatively limited body size diversity, but greater overall phenotypic
427 specialization for interaction with their flower resources (Stiles 1981; Fleming and Muchhala 2008;
428 Zanata et al. 2017). Fleming and Muchhala (2008) attributed the among-clade differences in
429 nectarivory specialization and body size diversity to variation in floral resource predictability
430 among major regions, ranging from highest in the Neotropics to comparatively low in Australia. In
431 concordance with this hypothesis, we suggest that strong competition for a valued resource, which
432 can be highly unpredictable in its spatial and temporal occurrence, has been the prominent driver of
433 body size evolution among the Australasian honeyeaters. In addition to increased rates of body size
434 evolution, the transition to a nectarivorous diet appears to have had a profound influence on bill
435 evolution among honeyeaters. Our results thus suggest that honeyeaters have unique bill
436 morphology (i.e. longer and narrower) compared to the background meliphagoids and other
437 regional passerines (Fig. S4; Table S6-7), whereas nectarivorous meliphagoid lineages are also
438 found to have a higher rate of bill (pPC4) evolution than non-nectarivorous lineages (Table 1).
439 Taken together, our results suggest that the evolution of nectarivory among honeyeaters have had
440 important consequences for both rates of morphological evolution (i.e. body size) and
441 morphological adaptations (i.e. bill size and shape) in this clade.

442 The extensive and continuous accumulation of morphological disparity among
443 honeyeaters relative to the background meliphagoids, could be caused in part by recent
444 morphological evolution into further novel and unoccupied areas of niche-space (Simpson 1944;
445 Slater 2015; Cooney et al. 2017). Examples of this include the genera *Macgregoria* and *Melipotes*
446 that have transitioned to a largely fruit-based diet that is also reflected in their generally shorter and

447 straighter bills relative to most other honeyeaters. Alternatively, this pattern could reflect the
448 outcome of strong ecological character displacement, whereby interspecific competition among
449 recently separated taxa selects for rapid phenotypic divergence (Brown and Wilson 1956; Schluter
450 2000b). Many island species such as the two sympatric New Zealand honeyeater taxa
451 *Prosthemadera* and *Anthornis* may represent an extreme example of this process, as they display
452 high levels of recent body size divergence, which is also consistent with the expectation of greater
453 character displacement among species in depauperate environments (Schluter 2000b). Thus, both
454 character displacement and diversification into further available and unoccupied niche space are
455 probable explanations that likely contributed to the continual accumulation of disparity in the case
456 of honeyeaters.

457 Although transitions into new adaptive zones (and adaptive radiation more generally)
458 need not always result in increased rates of lineage diversification, increases in ecological diversity
459 of the adaptively radiating clade may be predicted to facilitate the build-up of extensive sympatric
460 species diversity (Givnish 1997; Losos and Mahler 2010; Stroud and Losos 2016; Givnish 2015;
461 Rabosky 2017). Consistent with these predictions, we find that whereas there is no evidence of a
462 decoupling of diversification dynamics among nectarivorous and non-nectarivorous meliphagoid
463 lineages (Fig. S9; Table S5), the evolution of nectarivory appears to have influenced the build-up of
464 extensive sympatric species richness among the predominantly nectarivorous honeyeaters. Thus,
465 although honeyeaters and the other families within the Meliphagides share very similar
466 distributional extents and geographic diversity gradients (Fig. 3 and 4), honeyeaters exhibit much
467 higher levels of species richness within the same grid cells compared to that of the background
468 meliphagoids. Although honeyeaters might be expected to accumulate higher grid cell richness than
469 the background meliphagoids due to their higher overall species diversity, a null explanation such
470 as this is unlikely to be sufficient in accounting for the strong correlations between grid cell

richness, body-size disparity and the trends of trait evolution. The evolution of nectarivory among the honeyeaters may thus represent an intriguing example of how evolutionary innovations may positively influence the build-up of species diversity without necessarily having direct effects on rates of lineage diversification (Rabosky 2017).

A number of non-mutually exclusive mechanisms may underlie the increased sympatric species diversity of honeyeaters, including elevated ecological diversity (Keast 1976; Miller et al. 2017), and increased dispersal capabilities. The association between sympatric species richness and body size diversity recovered here suggest either that diversity drives ecological divergence by character displacement, or alternatively, that expansion into unoccupied niche space allows more species of honeyeaters to coexist through relaxed ecological filtering. Whereas substantial expansion in morphological space of other regional clades may have been constrained by the presence of ecologically similar lineages, honeyeaters appear to have been able to expand more freely due to the general absence of competing nectarivores. Although Australasia and the Indo-Pacific is inhabited by some other nectarivorous birds, including non-passerine parrots such as the lories and lorikeets (family Psittacidae: tribe Loriinae), this group is thought to have radiated considerably later than the honeyeaters, with most of the diversification having taken place in the last 5 million years (Schweizer et al. 2015). In comparison with honeyeaters, this group is characterized by comparatively low levels of sympatric species diversity (Schweizer et al. 2015), which could suggest that the ecological diversification of lories and lorikeets has itslef been constrained by the more ecologically diverse honeyeaters. Lories and lorikeets appear to be less ecologically diverse than honeyeaters, exhibiting a comparatively reduced diversity of bill shapes and adaptation to a narrower range of habitats, dietary resources and foraging modes. However, in the absence of detailed ecological and morphological data for the lories and lorikeets, these hypotheses necessitate formal testing. Finally, a number of nectarivorous bats also inhabit the

Australasian/Indo-Pacific region (family Pteropodidae), but as these are primarily nocturnal, direct competition with the diurnal honeyeaters is unlikely to have been pervasive.

Under a model of allopatric speciation, for character displacement to occur, genetic/reproductive differentiation must first accumulate in geographic isolation before subsequent range shifts into sympatry (Price 2008). The rate at which this process occurs is at least partly contingent on the dispersal propensity of the organisms in question, as this positively influences the rate at which lineages achieve range overlap (Pigot and Tobias 2015). A lack of positive selective pressures on factors that directly facilitate dispersal may thus help to explain why some adaptive radiations are notably species-poor (Losos and Mahler 2010; Givnish 2015). Among honeyeaters, good dispersal abilities are a well-established characteristic of many species and this is likely to have enabled frequent colonization and exchange between geographic regions (Keast 1968; Marki et al. 2017). The irregular, unpredictable and often highly disjunct occurrence of many nectar sources may have exposed honeyeaters to significant positive selection for increased dispersal capabilities as evidenced by the major seasonal and nomadic movements of many species (Keast 1968; Pyke 1980; Wooller 1981). Our findings support this, with honeyeaters having on average longer and more projected wing tips compared to background meliphagoids, suggesting high dispersal capacity (Fig. S13; Claramunt et al. 2012). Thus, increased dispersal abilities among the many nectar-dependent honeyeaters may have been an additional factor promoting the build-up of species diversity by increasing the rates at which new populations are founded, and their subsequent transitions back into sympatry following differentiation (Pigot and Tobias 2015).

The utilization of previously inaccessible resources has been hypothesized to underlie the adaptive radiation of a wide range of organismal groups. Here, we have shown that an ancestral shift to a nectarivorous diet is correlated with rapid body size evolution and the accumulation of extensive size disparity within the speciose radiation of Australasian honeyeaters. Importantly, our

findings suggest that the rapid invasion of novel and previously unoccupied ecological space can positively affect the build-up of species and functional diversity across different spatial scales, even in the presence of related and likely competing lineages. Overall, these results highlight the important role of ecological opportunity in facilitating the generation of morphological and species diversity across large geographic areas.

References

Barker, F. K., A. Cibois, P. Schikler, J. Feinstein, and J. Cracraft. 2004. Phylogeny and diversification of the largest avian radiation. Proc. Natl. Acad. Sci. USA. 101:11040–11045.

Beaulieu, J. M., and B. C. O'Meara. 2016. Detecting hidden diversification shifts in models of trait-dependent speciation and extinction. Sys. Bio. 65:583-601.

Blonder, B., C. Lamanna, C. Violle, and B. J. Enquist. 2014. The n- dimensional hypervolume. Glob. Ecol. Biogeogr. 23(5):595-609.

Blonder, B., D. Nogués-Bravo, M. K. Borregaard, I. I. Donoghue, C. John, P. M. Jørgensen, P.M. et al. 2015. Linking environmental filtering and disequilibrium to biogeography with a community climate framework. Ecology 96, 972–985.

Bollback, J. P. 2006. SIMMAP: stochastic character mapping of discrete traits on phylogenies. BMC Bioinformatics 7, 88.

539 Bond, J. E., and B. D. Opell. 1998. Testing adaptive radiation and key innovation hypotheses in
540 spiders. Evolution 52, 403-414.

541 Brown, W. L., and E. O. Wilson. 1956. Character displacement. Syst. Zool. 5:49–64.

542 Casotti, G., and K. C. Richardson. 1992. A stereological analysis of kidney structure of
543 honeyeater birds (Meliphagidae) inhabiting either arid or wet environments. J. Anat.
544 180:281.

545 Chira, A. M., and G. H. Thomas. 2016. The impact of rate heterogeneity on inference of
546 phylogenetic models of trait evolution. J. Evol. Biol. 29:2502-2518.

547 Claramunt, S., E. P. Derryberry, J. V. Remsen, and R. T. Brumfield. 2012. High dispersal
548 ability inhibits speciation in a continental radiation of passerine birds. Proc. Biol. Sci.
549 279:1567-1574.

550 Clavel, J., G. Escarguel, and G. Merceron. 2015. mvMORPH: and R package for fitting multivariate
551 evolutionary models to morphometric data. Methods Ecol. Evol. 6:1311-1319.

552 Cooney, C. R., J. A. Bright, E. J. R. Capp, A. M. Chira, E. C. Hughes, C. J. A. Moody, C.J.A. et al.
553 2017. Mega-evolutionary dynamic of the adaptive radiation of birds. Nature 542:344-
554 347.

555 Diamond, J.M. 1982. Mimicry of friarbirds by orioles. Auk 99:187–196.

556 Diamond, J., S. L. Pimm, M. E. Gilpin, and M. LeCroy. 1989. Rapid evolution of character
557 displacement in myzomelid honeyeaters. Am. Nat. 134:675-708.

558 Fleming, T.H., and N. Muchhala. 2008. Nectar-feeding bird and bat niches in two worlds:
559 pantropical comparisons of vertebrate pollination systems. J. Biogeogr. 35:764-780.

560 Futuyma, D. J. 1998. Evolutionary Biology Sinauer Associates, Sunderland, MA.

561 Galis, F., and E. G. Drucker. 1996. Pharyngeal biting mechanisms in centrarchid and cichlid
562 fishes: insights into a key evolutionary innovation. J. Evol. Biol. 9:641–670.

563 Gardner, J. L., and J. W. H. Trueman, D. Ebert, L. Joseph, and R. D. Magrath. 2010. Phylogeny and
564 evolution of the Meliphagoidea, the largest radiation of Australasian songbirds. Mol.
565 Phylogenet. Evol. 55:1087–1102.

566 Gill, F., and D. Donsker. 2016. IOC World Bird List (v 6.2). doi:10.14344/IOC.

567 Givnish, T. J. 1997. Adaptive radiation and molecular systematics: Issues and approaches. In
568 Molecular Evolution and Adaptive Radiation (eds Givnish, T.J., Sytsma, K.J.).
569 Cambridge University Press, Cambridge, UK, pp. 1-54.

570 Givnish, T. J. 2015. Adaptive radiation versus 'radiation' and 'explosive diversification': why
571 conceptual distinctions are fundamental to understanding evolution. New Phytol.
572 207:297-303.

573 Goldstein, D. L., and S. D. Bradshaw. 1998a. Regulation of water and sodium balance in the field
574 by Australian honeyeaters (Aves: Meliphagidae). Physiol. Zool. 71(2):214-225.

575 Goldstein, D. L., and S. D. Bradshaw. 1998b. Renal function in red wattlebirds in response to
576 varying fluid intake. J. Comp. Physiol. B, 168(4):265-272.

577 Grant, P. R., and B. R. Grant. 2008. How and Why Species Multiply: The Radiation of Darwin's
578 Finches Princeton University Press, Princeton, NJ.

579 Harmon, L. J., J. T. Weir, C. D. Brock, R. E. Glor, and W. Challenger. 2008. GEIGER:
580 investigating evolutionary radiations. Bioinformatics 24, 129-131.

581 Hodges, S.A., and M. L. Arnold. 1995. Spurring plant diversification: are floral nectar spurs a key
582 innovation?. Proc. R. Soc. Lond. B, 262, 343-348.

583 Hunter, J. P. 1998. Key innovations and the ecology of macroevolution. Trends. Ecol. Evol. 13, 31-
584 36.

585 Huxley, J. 1942. Evolution. The Modern Synthesis. Allen & Unwin, London.

586 Jønsson, K. A., P-H. Fabre, R. E. Ricklefs, and J. Fjeldså. 2011. Major global radiation of
587 corvoid birds originated in the proto-Papuan archipelago. Proc. Natl. Acad. Sci. USA.
588 108:2328-2333.

589 Keast, A. 1968. Seasonal movements in the Australian honeyeaters (Meliphagidae) and their
590 ecological significance. Emu 67:159-209.

591 Keast, A. 1976. The origins of adaptive zone utilizations and adaptive radiations, as illustrated by
592 the Australian Meliphagidae. Proceedings of the XVI International Ornithological
593 Congress 71-82.

594 Keast, A. (1985) An introductory ecological biogeography of the Australo-Pacific Meliphagidae.
595 New Zealand Journal of Zoology 12:605-622.

596 Liem, K. F. 1973. Evolutionary strategies and morphological innovations: cichlid pharyngeal jaws.
597 Syst. Zool. 22:425–44.

598 Losos, J. B. 2009. Lizards in an Evolutionary Tree: Ecology and Adaptive Radiation of Anoles
599 University of California Press, Berkeley, CA.

600 Losos, J. B. 2010. Adaptive radiation, ecological opportunity, and evolutionary determinism. Am.
601 Nat. 175:623-639.

602 Losos, J. B., and D. L. Mahler. 2010. Adaptive radiation: The interaction of ecological opportunity,
603 adaptation, and speciation. In Evolution Since Darwin: The First 150 Years (eds Bell,
604 M.A., Futuyma, D.J., Eanes, W.F., Levinton, J.S.), Sinauer Associates, Sunderland,
605 MA, pp. 381-420.

606 Maddison, W.P., P. E. Midford, and S. P. Otto. 2007. Estimating a binary character's effect on
607 speciation and extinction. Sys. Bio. 56:701-710.

608 Marki, P. Z., K. A. Jønsson, M. Irestedt, J. M. T. Nguyen, C. Rahbek, and J. Fjeldså. 2017.
609 Supermatrix phylogeny and biogeography of the Australasian Meliphagides radiation
610 (Aves: Passeriformes). Mol. Phylogenet. Evol. 107:516-529.

611 Miller, A. H. 1949. Some ecologic and morphologic considerations in the evolution of higher
612 taxonomic categories. In Ornithologie als Biologische Wissenschaft (eds E Mayr, E
613 Schüz), Carl Winter, Heidelberg, Germany, pp. 84-88.

614 Miller, E.T., S. K. Wagner, L. J. Harmon, and R. E. Ricklefs. 2017. Radiating despite a lack of
615 character: ecological divergence among closely related, morphologically similar
616 honeyeaters (Aves: Meliphagidae) co-occurring in arid Australian environments. Am.
617 Nat. 189:14-30.

618 Mitter, C., B. Farrell, and B. Wiegmann. 1988. The phylogenetic study of adaptive zones: has
619 phytophagy promoted insect diversification? Am. Nat. 132:107-128.

620 Moyle, R. G., C. H. Oliveros, M. J. Andersen, P. A. Hosner, B. W. Benz, J. D. Manthey, et al.
621 (2016) Tectonic collision and uplift of Wallacea triggered the global songbird
622 radiation. Nat. Commun. 7:12709.

623 Osborn, H. F. 1902. The law of adaptive radiation. Am. Nat. 36:353–363.

624 Paton, D. C. and B. G. Collins. 1989. Bills and tongues of nectar- feeding birds: A review of
625 morphology, function and performance, with intercontinental comparisons. Austral
626 Ecology, 14(4):473-506.

627 Paton, D. C., and H. A. Ford. 1983. The influence of plant characteristics and honeyeater size on
628 levels of pollination in Australian plants. In Handbook of Experimental Pollination
629 Biology (eds Jones, C.E., Little, R.J.), Van Nostrand-Reihold, Princeton, NJ, pp. 235-
630 248.

631 Pennell, M. W., R. G. FitzJohn, W. K. Cornwell, and L. J. Harmon. 2015. Model adequacy and the
632 macroevolution of angiosperm functional traits. Am. Nat. 186:E33-E50.

633 Pigot, A. L., and J. A. Tobias. 2015. Dispersal and the transition to sympatry in vertebrates. Proc.
634 Biol. Sci. 282:20141929.

635 Pratt, H. D. 2005. The Hawaiian Honeycreepers: Drepanididae Oxford University Press,
636 Oxford, UK.

637 Price, T. 2008. Speciation in Birds. Roberts and Co, Boulder, CO.

638 Prum, R. O. 2014. Interspecific social dominance mimicry in birds. Zool. J. Linn. Soc. 172:910-
639 941.

640 Pyke, G. H. 1980. The foraging behaviour of Australian honeyeaters: a review and some
641 comparisons with hummingbirds. Australian Journal of Ecology 5:343-369.

642 Rabosky, D. L. 2014. Automatic detection of key innovations, rate shifts, and diversity-
643 dependence on phylogenetic trees. PLoS One 9:e89543.

644 Rabosky, D. L. 2017. Phylogenetic tests for evolutionary innovation: the problematic link
645 between key innovations and exceptional diversification. Phil. Trans. R. Soc.
646 372:20160417.

647 Rabosky, D. L., S. C. Donnellan, M. Grundler, and I. J. Lovette. 2014a. Analysis and visualization
648 of complex macroevolutionary dynamics: an example from Australian scincid lizards.
649 Syst. Bio. 63:610-627.

650 Rabosky, D. L., and E. E. Goldberg. 2015. Model inadequacy and mistaken inferences of trait-
651 dependent speciation. Sys. Bio. 64:340-355.

652 Rabosky, D. L., M. Grundler, C. Anderson, P. Title, J. J. Shi, J. W. Brown, et al. 2014b.
653 BAMMtools: and R package for the analysis of evolutionary dynamics on phylogenetic
654 trees. Methods Ecol, Evol, 5:701-707.

655 Rahbek, C., and G. R. Graves. 2001. Multiscale assessment of patterns of avian species richness.
656 Proc. Natl. Acad. Sci. USA 98:4534–4539.

657 Rahbek, C., L. A. Hansen, and J. Fjeldså. 2012. Data from "One degree resolution database of the
658 global distribution of birds." The Natural History Museum of Denmark, Univ. of
659 Copenhagen, Denmark. http://macroecology.ku.dk/resources/.

660 R Core Team. 2016. R: A language and environment for statistical computing. R Foundation for
661 Statistical Computing, Vienna, Austria. URL https://www.R-project.org/.

662 Revell, L. J. 2009. Size-correction and principal components for interspecific comparative studies.
663 Evolution 63:3258-3268.

664 Revell, L. J. 2012. Phytools: An R package for phylogenetic comparative biology (and other
665 things). Methods Ecol. Evol. 3:217-223.

666 Schluter, D. 1996. Ecological causes of adaptive radiation. Am. Nat. 148:S40–S64.

667 Schluter, D. 2000a. The Ecology of Adaptive Radiation. Oxford University Press, Oxford, UK.

668 Schluter, D. 2000b. Ecological character displacement in adaptive radiation. Am. Nat. 156:S4-S16.

669 Schweizer, M., T. F. Wright, J. V. Peñalba, E. E. Schirtzinger, L. Joseph. 2015. Molecular
670 phylogenetics suggest a New Guinean origin and frequent episodes of founder-event
671 speciation in the nectarivorous lories and lorikeets (Aves: Psittaciformes). Mol.
672 Phylogenet. Evol. 90:34-48.

673 Simpson, G. G. 1944. Tempo and Mode in Evolution. Columbia University Press, New York, NY.

674 Simpson, G. G. 1953. The Major Features of Evolution. Columbia University Press, New York,
675 NY.

676 Slater, G. J. 2015. Iterative adaptive radiations of fossil canids show no evidence for diversity-
677 dependent trait evolution. Proc. Natl. Acad. Sci. USA. 201403666.

678 Slowinski, J.B., and C. Guyer. 1993. Testing whether certain traits have caused amplified
679 diversification: an improved method based on a model of random speciation and
680 extinction. Am. Nat. 142, 1019-1024.

681 Soulebeau, A., X. Aubriot, M. Gaudeul, G. Rouhan, S. Hennequin, T. Haevermans, et al. 2015.
682 The hypothesis of adaptive radiation in evolutionary biology: hard facts about a hazy
683 concept. Org. Divers. Evol. 15:747-761.

684 Stiles, F. G. 1981. Geographical aspects of bird-flower coevolution, with particular reference to
685 Central America. Ann. Mo. Bot. Gard. 68:323–351.

686 Stroud, J. T., and J. B. Losos. 2016. Ecological opportunity and adaptive radiation. Annu. Rev.
687 Ecol. Evol. Syst. 47:507-532.

688 Venditti, C., A. Meade, and M. Pagel. 2011. Multiple routes to mammalian diversity. Nature
689 479:393-396.

690 Wallace, A. R. 1869. The Malay Archipelago. Dover Publication, New York, NY.

691 Wilman, H., J. Belmaker, J. Simpson, C. de la Rosa, M. M. Rivadeneira, and W. Jetz. 2014.
692 EltonTraits 1.0: Species- level foraging attributes of the world's birds and mammals.
693 Ecology 95:2027.

694 Wooller, R. D. 1981. Seasonal changes in a community of honeyeaters in southwestern
695 Australia. Emu 81:50-51.

696 Zanata, T. B., B. Dalsgaard, F. C. Passos, P. A. Cotton, J. J. Roper, P. K. Maruyama, et al.
697 2017. Global patterns of interaction specialization in bird–flower networks. J.
698 Biogeogr. 44(8):1891-1910.

699

700

701

702

703

Tables

Table 1. Comparisons of evolutionary models testing for a decoupling of rates of trait evolution between nectarivorous and non-nectarivorous lineages. The best-fitting models are highlighted in bold. Shown are the mean and standard deviations of delta AICc values, AICc weights, and Brownian variance (σ^2) as estimated across 1,000 (univariate analyses of pPC1-4) and 10 (multivariate analysis of pPC1-4) stochastic character maps of the evolutionary history of diets among the Meliphagides.

	pPC1	pPC2	pPC3	pPC4	pPC1-4
BM1					
Delta AICc	7.8±1.8	8.5±1.1	**0.00±0.00**	9.1±1.9	17.1±3.8
AICc weight	0.03±0.02	0.02±0.01	**0.71±0.02**	0.02±0.02	0.00±0.00
σ^2	0.022±0.000	0.007±0.000	**0.002±0.000**	0.001±0.000	0.032±0.000
BMM					
Delta AICc	**0.0±0.0**	**0.0±0.0**	1.8±0.2	**0.0±0.0**	**0.0±0.0**
AICc weight	**0.97±0.03**	**0.98±0.01**	0.29±0.02	**0.98±0.02**	**1.00±0.00**
σ^2 (nectarivorous)	**0.026±0.000**	**0.005±0.000**	0.002±0.000	**0.002±0.000**	**0.035±0.000**
σ^2 (non-nectarivorous)	**0.014±0.001**	**0.009±0.000**	0.002±0.000	**0.001±0.000**	**0.026±0.001**

720 **Supplementary tables**

721 Table S1. Description of morphological traits measured using a calliper and taken to the nearest 0.1
722 mm (tarsus, hind toe and bill measurements), or using a wing ruler taken to the nearest 1 mm (wing
723 length and Kipp's distance).

Trait	Description
Tarsus length	Length of the tarsometatarsus as measured from the tibiotarsus joint to the base of the toes, which is represented by the last undivided scute.
Hind toe	Length of the hallux and claw as measured on dorsal side.
Bill length	Total culmen length as measured from the tip of bill to the base of the skull
Bill depth	Vertical height of the bill as measured at the proximal edge of the nostrils
Bill width	Horizontal width of bill as measured at the proximal edge of the nostrils
Wing length	Length of the wing as measured from the carpal joint to the longest primary measured on a flattened wing.
Kipp's distance	The difference in wing length as measured above, and the length from the carpal joint to the first secondary feather measured on a flattened wing

724

725

726

727

728

729

730

731

Table S2. Correlation coefficients and proportion of variance explained by each of the phylogenetic principal component (pPC) axes for the analysis of the Meliphagides dataset (n = 273 species).

Trait	pPC1	pPC2	pPC3	pPC4	pPC5	pPC6	pPC7
Tarsus length	-0.869	0.212	0.237	-0.246	-0.042	-0.279	0.066
Hind toe	-0.862	0.294	0.316	-0.110	0.055	0.229	0.051
Bill length	-0.794	0.349	0.114	0.477	0.030	-0.071	0.008
Bill depth	-0.832	0.222	-0.452	-0.076	0.219	-0.006	0.027
Bill width	-0.812	0.277	-0.330	-0.009	-0.386	0.072	0.028
Wing length	-0.955	-0.056	0.058	-0.077	-0.005	-0.008	-0.276
Kipp's distance	-0.678	-0.733	0.003	0.040	-0.004	0.009	0.036
Proportion of variance	0.653	0.196	0.063	0.039	0.022	0.018	0.009
Cumulative proportion of variance	0.653	0.849	0.912	0.951	0.973	0.991	1.000

Table S3. Trait loadings and proportion of variance explained by each of the principal component axes for the analysis of the full passerine dataset (n = 671 species).

Trait	PC1	PC2	PC3	PC4	PC5	PC6	PC7
Tarsus length	0.240	0.373	-0.338	0.511	0.214	-0.604	-0.130
Hind toe	0.306	0.325	-0.311	0.239	-0.380	0.633	-0.320
Bill length	0.345	0.275	-0.306	-0.816	-0.009	-0.197	-0.082
Bill depth	0.433	0.212	0.479	0.004	0.671	0.289	-0.058
Bill width	0.346	0.081	0.642	0.030	-0.582	-0.322	-0.134
Wing length	0.373	0.043	-0.107	0.104	-0.137	0.080	0.901
Kipp's distance	0.531	-0.791	-0.205	0.066	0.054	-0.045	-0.202
Proportion of variance	0.822	0.117	0.029	0.018	0.007	0.004	0.003
Cumulative proportion of variance	0.822	0.939	0.968	0.986	0.993	0.997	1.000

745 Table S4. Comparison of model fit for different models of morphological evolution. Delta log-
746 likelihoods values are shown for alternative models of morphological evolution. Values for the
747 BayesTraits and BAMM were generated by estimating the likelihoods of a BM model fit to the
748 mean rate-transformed trees.

	pPC1	pPC2	pPC3	pPC4
BayesTraits	0.0	0.0	0.0	0.0
BAMM	32.9	33.1	28.3	32.9
BM	65.8	47.4	85.1	66.8
OU	65.8	47.4	61.4	66.8
EB	65.8	47.4	85.1	66.8

749

750 Table S5. Comparisons of lineage diversification models using HiSSE.

Model	**Parameter constraints**	**No. of parameters**	**Delta AICc**	**AICc weight**
BiSSE null	Speciation, extinction and transition rates equal	3	5.3	0.05
HiSSE 1	Transition rates equal	5	2.1	0.24
HiSSE 2	**Extinction and transition rates equal**	**4**	**0**	**0.67**
BiSSE 1	Transition rates equal	5	8.0	0.01
BiSSE 2	Extinction and transition rates equal	4	6.0	0.03

751

752 Table S6. Normalized canonical coefficients separating honeyeaters and other regional passerines
753 on the basis of the seven original log-transformed variables.

Trait	**Tarsus**	**Hind toe**	**Bill length**	**Bill depth**	**Bill width**	**Wing length**	**Kipp's distance**
Coefficient	1.141	0.564	-5.525	-0.519	5.842	0.760	-0.932

754

755 Table S7. Classification of passerine species based on the linear discriminant analysis.

Family	Acanthizidae	Artamidae	Campephagidae	Cinclosomatidae	Climacteridae	Corvidae	Dasyornithidae	Maluridae	Melanocharitidae	Meliphagidae	Monarchidae	Oriolidae	Pachycephalidae	Paradisaeidae	Pardalotidae	Petroicidae	Ptilonorhynchidae	Rhipiduridae	Total number of species	Classification accuracy
Acanthizidae	51	0	0	0	0	0	1	6	0	1	1	0	2	0	0	0	0	0	62	0.82
Artamidae	0	17	2	0	0	4	0	0	0	0	0	0	0	0	0	0	0	0	23	0.74
Campephagidae	0	2	39	0	0	0	0	0	0	3	0	0	1	0	0	3	0	0	48	0.81
Cinclosomatidae	1	0	0	4	0	0	2	0	0	2	0	0	1	0	0	1	0	0	11	0.36
Climacteridae	0	0	0	0	7	0	0	0	0	0	0	0	0	0	0	0	0	0	7	1.00
Corvidae	0	0	0	0	0	18	0	0	0	0	0	0	0	0	0	0	0	0	18	1.00
Dasyornithidae	0	0	0	0	0	0	3	0	0	0	0	0	0	0	0	0	0	0	3	1.00
Maluridae	7	0	0	0	0	0	3	14	0	0	0	0	0	0	0	0	0	0	24	0.58
Melanocharitidae	2	0	0	0	0	0	0	0	0	4	2	0	0	0	0	1	0	0	9	0.00
Meliphagidae	2	0	1	0	0	1	0	0	0	161	1	0	2	4	0	6	0	2	180	0.89
Monarchidae	0	0	0	0	0	0	0	0	0	7	50	0	4	0	0	2	0	3	66	0.76
Oriolidae	0	1	6	0	0	0	0	0	0	0	2	6	1	0	0	0	2	0	18	0.33
Pachycephalidae	0	0	0	0	0	0	0	1	0	2	2	0	41	0	0	0	1	1	48	0.85
Paradisaeidae	0	0	0	0	0	0	0	0	0	6	0	1	0	33	0	1	0	0	41	0.80
Pardalotidae	0	0	0	0	0	0	0	0	0	0	0	0	0	0	4	0	0	0	4	1.00
Petroicidae	2	0	1	4	0	0	0	1	0	2	7	0	0	0	0	27	0	4	48	0.56
Ptilonorhynchidae	0	0	0	0	0	0	0	0	0	0	0	0	2	0	0	2	21	0	25	0.84
Rhipiduridae	0	0	1	0	0	0	0	0	0	1	6	0	0	0	0	6	0	22	36	0.61

756

757

758

Table S8. Comparisons of evolutionary models testing for a decoupling of rates of trait evolution between nectarivorous and non-nectarivorous lineages that accounted for phylogenetic uncertainty. The best-fitting models are highlighted in bold. Shown are the mean and standard deviations of delta AICc values, AICc weights, and Brownian variance (σ^2) as estimated across 1,000 (univariate analyses of pPC1-4) and 10 (multivariate analysis of pPC1-4) stochastic character maps of the evolutionary history of nectarivorous diet among the Meliphagides. The character maps were generated by running a single simulation across each tree in the posterior distribution of 1,000 trees obtained from the study of Marki et al. (2017).

	pPC1	pPC2	pPC3	pPC4	pPC1-4
BM					
Delta AICc	7.9±3.7	16.0±33.9	**1.4±8.9**	9.8±6.0	21.7±21.2
Akaike weight	0.06±0.11	0.05±0.06	**0.59±0.20**	0.04±0.11	0.05±0.12
σ2	0.023±0.003	0.008±0.006	**0.002±0.001**	0.001±0.000	0.035±0.005
BMM					
Delta AICc	**0.0±0.2**	**0.0±0.0**	1.2±0.8	**0.0±0.2**	**0.0±0.0**
Akaike weight	**0.94±0.11**	**0.95±0.06**	0.40±0.20	**0.96±0.11**	**0.95±0.12**
σ2 (nectarivorous)	**0.028±0.003**	**0.005±0.001**	0.002±0.001	**0.002±0.000**	**0.037±0.004**
σ2 (non-nectarivorous)	**0.015±0.003**	**0.012±0.016**	0.002±0.001	**0.001±0.000**	**0.030±0.006**

775 **Figure legends**

776 Figure 1. Diet and body size evolution among the Meliphagides. (*a*) Phylogeny of the Meliphagides
777 with ancestral estimation of the presence (red) or absence (yellow) of nectar in the diet.
778 Reconstructions were performed using stochastic character mapping and summarized using the
779 function *densityMap* in the R package phytools. *(b*) The phylogeny with branch lengths scaled by
780 the mean rate of body size (pPC1) evolution as estimated using the variable-rates model in
781 BayesTraits. Branch coloring reflects the relative rate of evolution. *(c*) Accumulation of size
782 disparity through time for the overall radiation (black), honeyeaters (red) and background
783 meliphagoids (blue). The black triangles show the stem branch of honeyeaters. Illustrations are
784 watercolors by Jon Fjeldså showing (clockwise from top) crow honeyeater (*Gymnomyza aubryana*),
785 mao (*Gymnomyza samoensis*), Meyer's friarbird (*Philemon meyeri*), cardinal myzomela (*Myzomela*
786 *cardinalis*) white-throated grasswren (*Amytornis woodwardi*), variegated fairywren (*Malurus*
787 *lamberti*), large-billed gerygone (*Gerygone magnirostris*), white-browed scrubwren (*Sericornis*
788 *frontalis*), western spinebill (*Acanthorhynchus superciliosus*), tui (*Prosthemadera*
789 *novaeseelandiae*), gibberbird (*Ashbyia lovensis*), MacGregor's honeyeater (*Macgregoria pulchra*),
790 orange-cheeked honeyeater (*Oreornis chrysogenys*), and Belford's melidectes (*Melidectes belfordi*).

791

792 Figure 2. Morphospace of Australasian passerine birds. Morphological diversity of honeyeaters (*n* =
793 180 species) (*a, b*) compared to that of the four background meliphagoid families (*n* = 93 species),
794 as well as 13 additional Australasian passerine families (*n* = 398 species) (c*, d*) as visualized using
795 the four first axes of variation from a phylogenetic and standard principal component analysis,
796 respectively. Principal components for the two sets of comparisons were generated separately.

797

798 Figure 3. Spatial diversity patterns of honeyeaters compared to that of background meliphagoids in
799 1° × 1° grid cells. Comparisons between honeyeaters (left) and background meliphagoids (right) for
800 differences in species richness (*a*), range and standard deviation of pPC1 (*b* and *c*) are shown.

801

802 Figure 4. Results of linear models examining the relationships between spatial diversity patterns.
803 The panels show the relationships between (*a*) grid cell richness of the honeyeaters and background
804 meliphagoids, grid cell richness of both groups and their range (*b*) or standard deviation (*c*) of
805 pPC1. Points represent the values in each 1° × 1° grid cell. Line in (*a*) is the 1:1 line, whereas lines
806 in (*b*) and (*c*) are the least-squares regression fits.

807

808

809

810

811

812

813

814

815

816

817

818

819

820

821 **Supplementary figure legends**

822 Figure S1. Mean shift configurations of BAMM analysis of pPC1-4.

823

824 Figure S2. Pairwise plots showing the estimated four-dimensional pPC hypervolumes for
825 honeyeaters (red points) and background meliphagoids (blue). Solid points reflect the empirical
826 data, whereas translucent points represent the stochastic points sampled from the estimated
827 hypervolumes. Large points represent the hypervolume centroids.

828

829 Figure S3. Pairwise plots showing the estimated four-dimensional pPCA hypervolumes for
830 honeyeaters (red points) and regional passerines (blue). Solid points reflect the empirical data,
831 whereas translucent points represent the stochastic points sampled from the estimated
832 hypervolumes. Large points represent the hypervolume centroids.

833

834 Figure S4. Distribution of discriminant scores for honeyeaters (top panel) and other regional
835 passerines (bottom panel). Large negative scores reflect species with long and narrow (width) bills,
836 and characterize honeyeaters relative to other groups.

837

838 Figure S5. Results from the BayesTraits variable-rates analysis of pPC1-4. Branch lengths are
839 scaled by the mean rate of evolution with branch coloring reflecting the relative rate of evolution.
840 Colored circles show rate shifts on individual internal branches, whereas colored triangles indicate

support for a whole-clade shift in rate of trait evolution. The relative size of the circles and triangles indicate the support (posterior probability) for a rate shift.

Figure S6. Accumulation of morphological disparity through time (pPC1-4) for the Meliphagides (solid black line), with separate lines for the honeyeaters (solid red line) and background meliphagoids (solid blue line). Shading shows the expected accumulation under a constant-rate BM model of trait evolution.

Figure S7. Accumulation of morphological disparity through time (pPC1-4) for the Meliphagides (solid black line), with separate lines for the honeyeaters (solid red line) and background meliphagoids (solid blue line). Shading shows the expected accumulation under a variable-rates model of trait evolution.

Figure S8. Phenograms of morphological disparity through time (pPC1-4) for the Meliphagides with separate coloration for the honeyeaters (red) and background meliphagoids (black).

Figure S9. Model-averaged speciation rates among the Meliphagides as inferred using the hidden-state speciation and extinction (HiSSE) framework. Ancestral estimation of diet is represented by white and black branches for nectarivorous and non-nectarivorous lineage respectively. The inset histogram shows the density distribution of speciation rates in the phylogeny.

862 Figure S10. Spatial diversity patterns of honeyeaters compared to that of background meliphagoids
863 in 1° × 1° grid cells. Comparisons between honeyeaters (left) and background meliphagoids (right)
864 for differences in the range and standard deviation of pPC2-4 are shown.

865

866 Figure S11. Spatial diversity patterns of honeyeaters compared to that of background meliphagoids
867 in 1° × 1° grid cells. Comparisons between honeyeaters (left) and background meliphagoids (right)
868 for differences in the 95% quantile range of pPC2-4 are shown.

869

870 Figure S12. Results of linear models examining the relationships between spatial diversity patterns.
871 The panels show the relationship between species richness and range (left) and standard deviations
872 (right) of pPC2-4 for each of the two groups. Points represent 1° × 1° grid cell values. Lines are the
873 least-squares regression fits.

874

875 Figure S13. Relationship between pPC2 and the log-transformed Kipp's distance values.

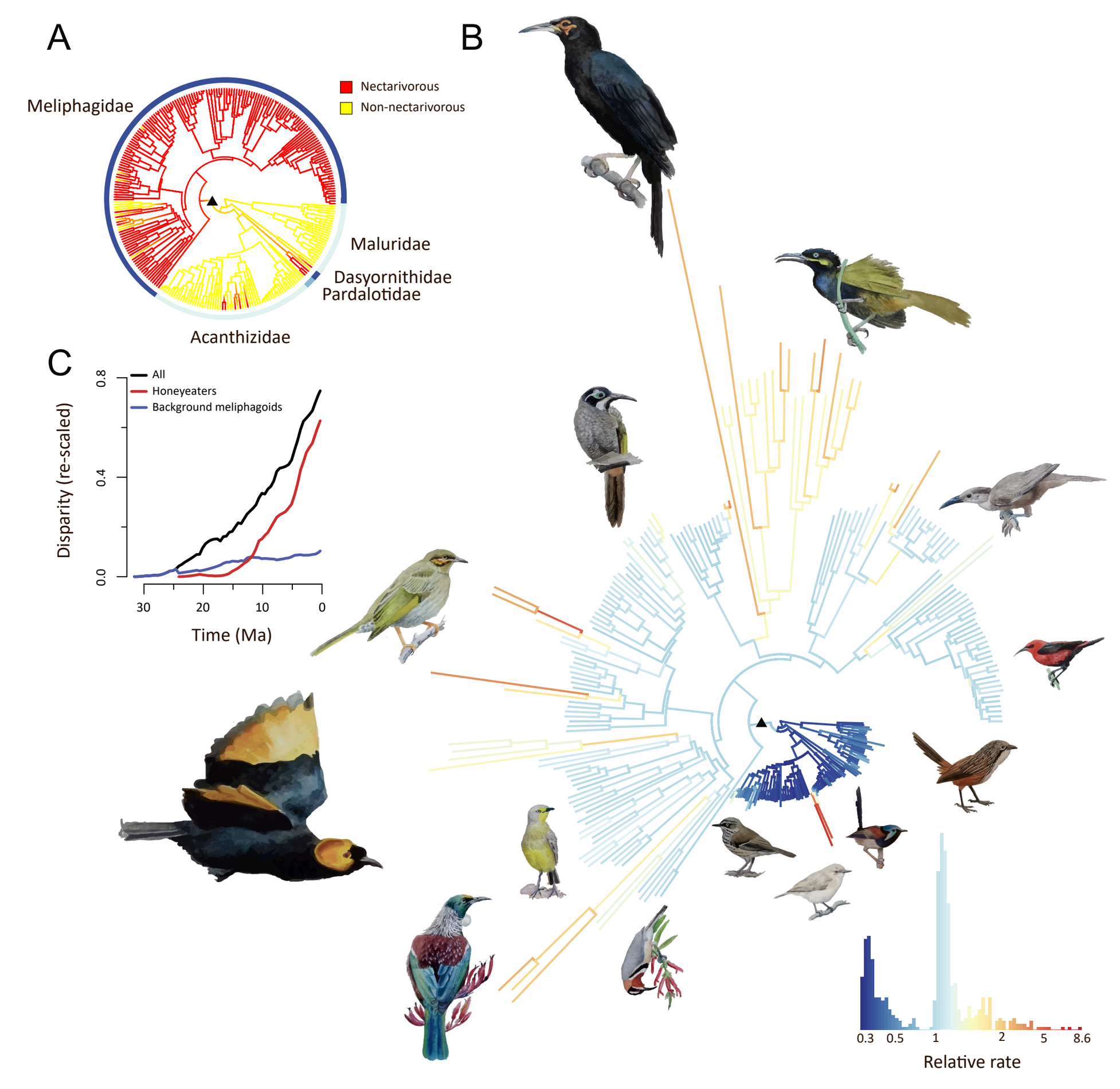
A
Meliphagidae
Nectarivorous
Non-nectarivorous
Maluridae
Dasyornithidae
Pardalotidae
Acanthizidae
B
C
All
Honeyeaters
Background meliphagoids
Disparity (re-scaled)
0.0
0.4
0.8
30
20
10
0
Time (Ma)
0.3
0.5
1
2
5
8.6
Relative rate

A

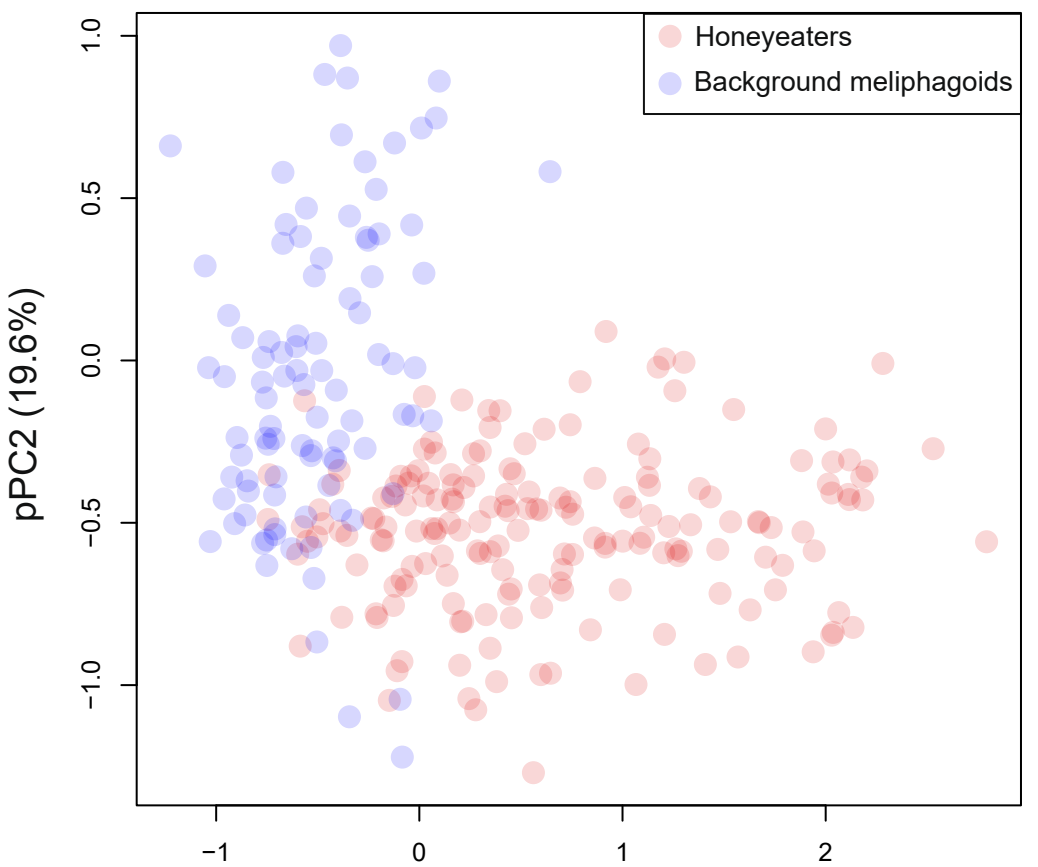
Honeyeaters
Background meliphagoids
pPC2 (19.6%)
1.0
0.5
0.0
−0.5
−1.0
−1
0
1
2

B

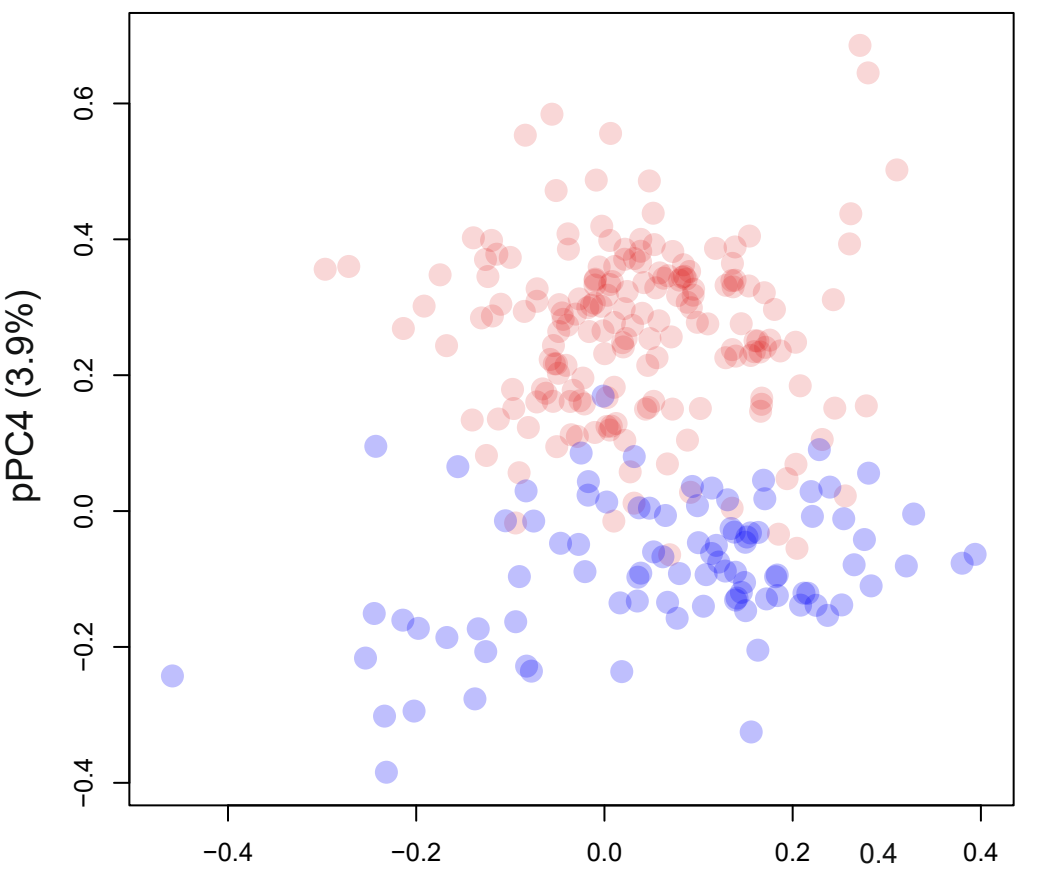
pPC4 (3.9%)
0.6
0.4
0.2
0.0
−0.2
−0.4
−0.4
−0.2
0.0
0.2
0.4
0.4

C

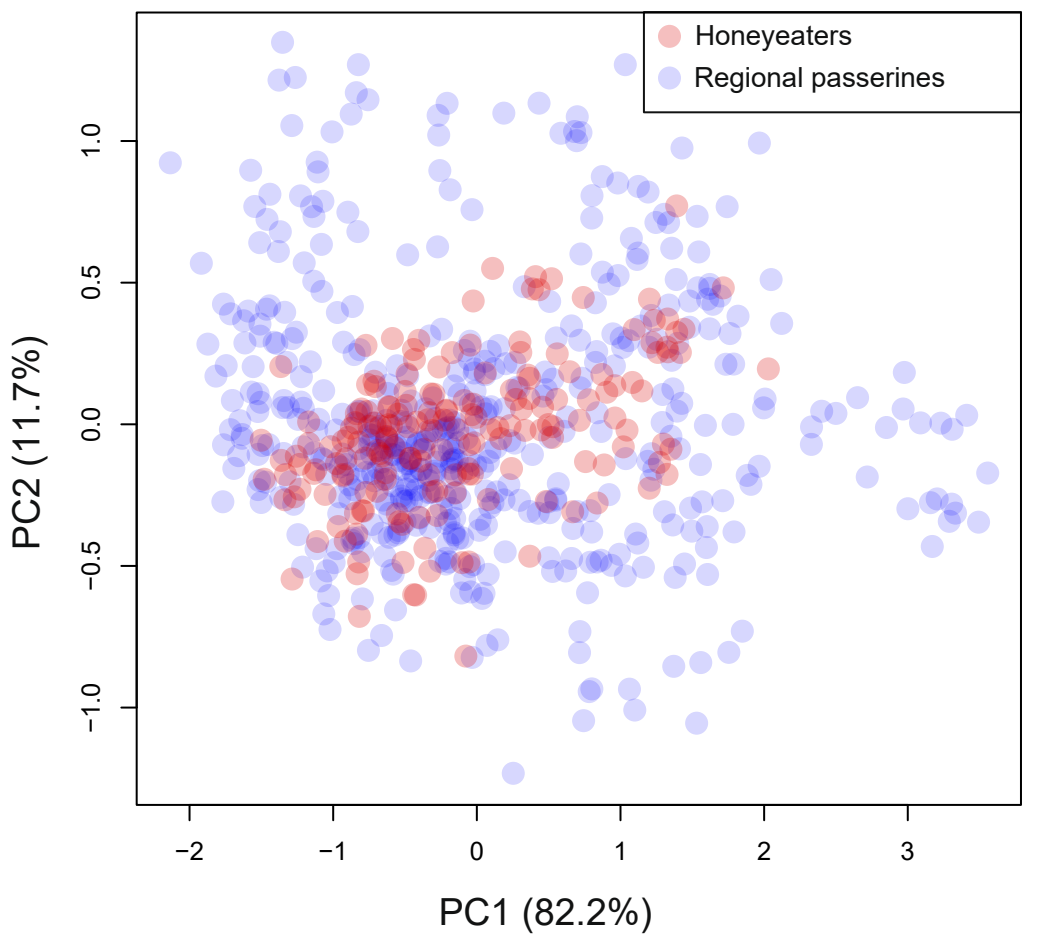
pPC1 (65.3%)
Honeyeaters
Regional passerines
PC2 (11.7%)
1.0
0.5
0.0
−0.5
−1.0
−2
−1
0
1
2
3
PC1 (82.2%)

D

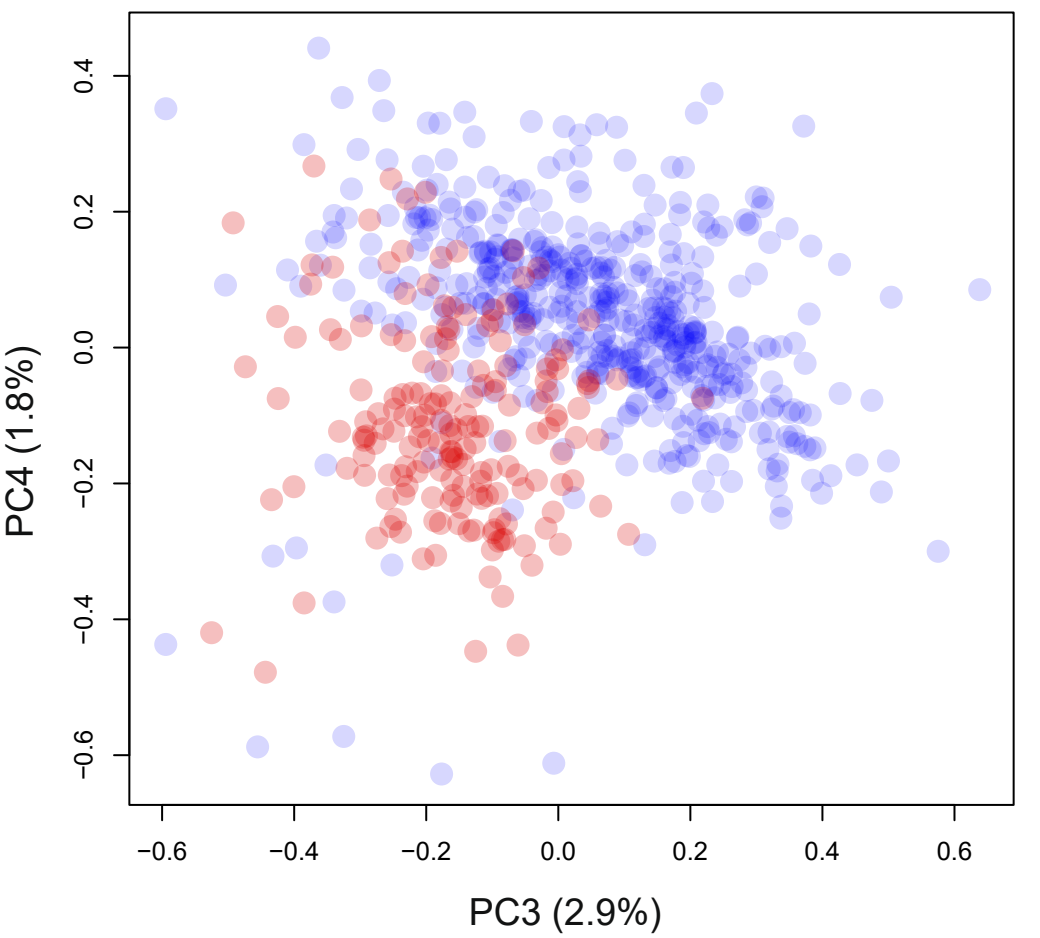
pPC3 (6.3%)
PC4 (1.8%)
0.4
0.2
0.0
−0.2
−0.4
−0.6
−0.6
−0.4
−0.2
0.0
0.2
0.4
0.6
PC3 (2.9%)

Honeyeaters

Background meliphagoids

A

Species richness

41

1

B

Range of pPC1

3.11

0.01

C

SD of pPC1

1.98

0

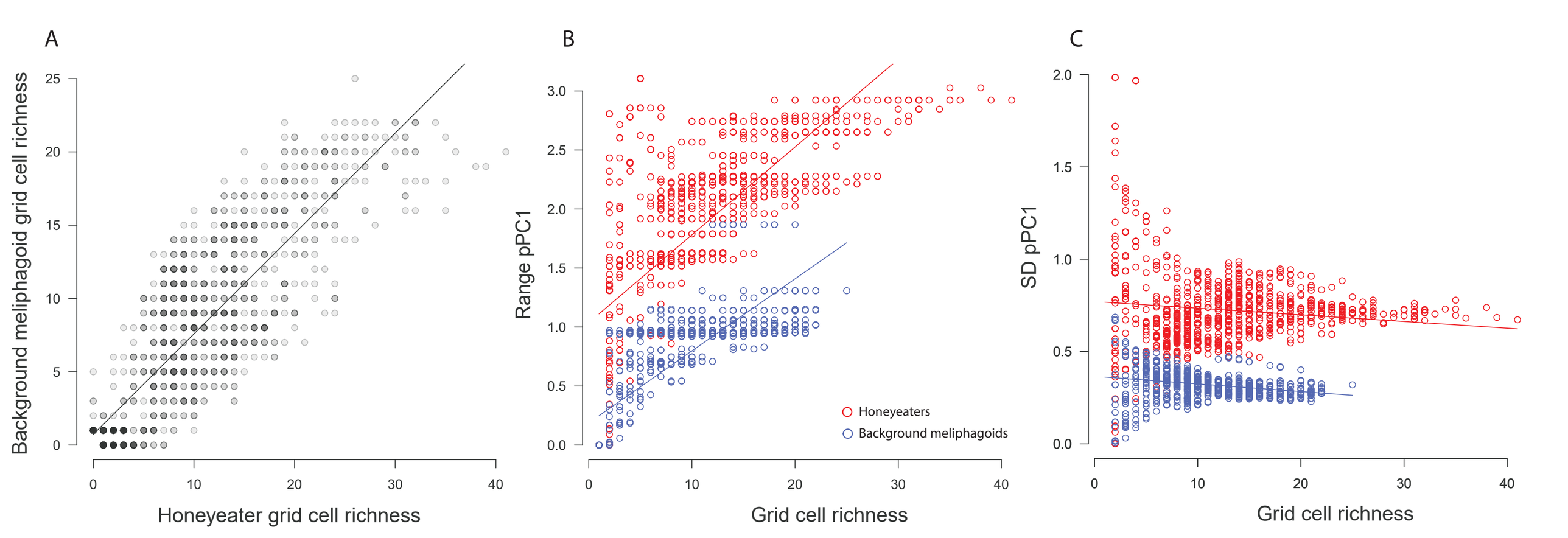
A
Background meliphagoid grid cell richness
Honeyeater grid cell richness
B
Range pPC1
Grid cell richness
Honeyeaters
Background meliphagoids
C
SD pPC1
Grid cell richness